ORIGINAL PAPER

Silicomolybdate doped polypyrrole film modified glassy carbon electrode for electrocatalytic reduction of Cr(VI)

A. Balamurugan · Shen-Ming Chen

Abstract Electrically conducting polypyrrole (PPy) film doped with silicomolybdate ($SiMo_{12}O_{40}^{4-}$ or $SiMo_{12}$) was synthesized by electrochemical polymerization. The synthesized film is capable of fast charge propagation during redox reactions in strong acid medium 0.2 M H_2SO_4 solution. Electrochemical quartz crystal microbalance was used to study the mechanism and amount of $SiMo_{12}$ doped in the PPy matrix. The modified electrode surface was characterized by using atomic force microscope technique, and it was found that the minimum and maximum globule size were estimated to be in the range of 50–200 nm. The thickness of film was measured to be approximately 30 ± 10 nm. The modified electrode shows electrocatalytic activity towards reduction of Cr(VI) and periodate. The rate constant and optimal film thickness were determined for electrocatalytic reduction of Cr(VI) by using rotating disc electrode experiment. Analytical characterization of the $SiMo_{12}$ doped PPy film modified electrode was demonstrated by flow injection analysis (FIA) technique and shows good stability for 16 continuous injections for Cr(VI) reduction with RSD of 1.6%.

Keywords PPy · Silicomolybdate · FIA · Electrocatalysis · Electrochemical polymerization

A. Balamurugan · S.-M. Chen (✉)
Electroanalysis and bioelectrochemistry lab, Department of Chemical Engineering and Biotechnology, National Taipei University of Technology,
No. 1, section 3, Chung-Hsiao East Road,
Taipei, Taiwan 106, Republic of China
e-mail: smchen78@ms15.hinet.net

Introduction

Chromium contamination of soil and groundwater is one of the significant environmental problems today. Chromium is believed to be the third most common pollutant at hazardous wastes sites, as well as the second most common inorganic contaminant after lead [1]. Chromium exists in the environment in either the trivalent Cr(III) or hexavalent Cr(VI) forms. Chromium(III) is considered to be essential to mammals for the maintenance of glucose, lipid, and protein metabolism. On the other hand, Cr(VI) is known to have adverse effects on the lungs, liver, and kidneys. The toxicity of chromium does not reside solely with the elemental form but varies greatly among a wide variety of chromium compounds. Oxidation state and solubility are crucial factors in this regard [2]. Hence, reduction of Cr(VI) to Cr(III) prior to discharge is considered to be an important step towards minimizing chromium pollution. There have been several studies on the methods and possible mechanisms of reduction of hexavalent chromium. Many industries treat chromium wastewater by aerobic or anaerobic, precipitation or ion exchange methods [3]. Other methods such as adsorption [4] and reverse osmosis [5] were used for chromium removal. Various reductants have been used so far for the reduction of Cr(VI), including iron [6], hydrogen peroxide [7], hydrogen sulfide [8], and thiols [9]. In addition, the chromium(VI) reduction process has also been studied with iron-reducing bacteria [10]. Furthermore, sol-gel materials prepared from organically modified silanes are used for sequestration and reduction of chromium(VI) [11]. More of these reducing agents have some limitations, such as low activity for reduction of total chromium(VI) at short period time. Furthermore, those reductants will cause second pollution in the remediations. Consequently, development of new strategies or methods of

converting toxic chromium wastes into nontoxic or less toxic compounds is critical in chromium remediation.

An alternative for the chemical reduction schemes currently employed for Cr(VI) treatment is an electrochemical reduction scheme. It is a promising technique that offers several advantages over other techniques for the transformation of Cr(VI) to essentially nontoxic Cr(III). Moreover, the electrochemical form of remediation offers a terminal process for recovery of metals from contaminated effluents or wastewaters [12, 13]. Direct electrolysis of Cr(VI), however, suffers from poor electron transfer kinetics, electrode passivation, and selectivity problems [14, 15]. The use of a mediator redox couple can decrease these difficulties, and in fact, an electrocatalytic reaction has been exploited commercially for Cr(VI) treatment [16, 17]. Polypyrrole (PPy), polyaniline, and poly(4-vinylpyridine) modified electrodes have been used for electrocatalytic reduction of Cr(VI) [18–20]. Due to the reversible electron transfer properties of $SiMo_{12}$, it can be used as an electron transfer mediator for electrocatalytic reduction of chromium.

Polyoxometalates (POMs) are promising candidates for the fabrication of new electrochromic or electrocatalytic devices, as well as magnetic devices [21, 22], owing to their well-defined structure, and they have the ability to undergo multielectron reversible redox reactions. Attachment of POMs to electrode surfaces can be achieved by electrode-position, adsorption, entrapment into polymers matrixes, self assembly and layer-by-layer deposition, sol-gel methods, and other strategies [23–28]. Different types of POMs-modified electrodes have been reported to study the electrocatalytic effect of chlorate, bromate, hydrogen peroxide, and nitrite by several groups [29–35] and determination of biomolecules like dopamine, creatinine etc. [36–38].

In this paper, $SiMo_{12}$ doped PPy film modified glassy carbon electrode was prepared by using repetitive cyclic voltammetry. Basic electrochemical characterization of this modified electrode and their electrocatalytic activity towards reduction of Cr(VI) and periodate was studied.

Experimental

All the chemicals used were of analytical grade and used without further purification. The aqueous solutions were prepared using doubly distilled deionized water and then deaerated by purging with high-purity nitrogen gas for about 20 min before performing electrochemical experiments. Also, a continuous flow of nitrogen over the aqueous solution was maintained during measurements.

The electrochemical experiments were carried out with a CH Instruments (Austin, TX, USA) (Model CHI-400) using CHI-750 potentiostat. Cyclic voltammograms (CVs) were recorded in a three-electrode-cell configuration, in which

BAS (West Lafayette, IN, USA) glassy carbon electrode (area = 0.07 cm^2) was used as working electrode. The auxiliary compartment contained a platinum wire that was separated by a medium-sized glass frit. All cell potentials were recorded using an Ag|AgCl|KCl (saturated solution). Rotating disc electrode (RDE) and amperometric experiments were performed using PINE Instruments (Grove City, PA, USA) in conjunction with CHI-750 potentiostat connected to a model AFMSRX analytical rotator. The RDE consisted of a glassy carbon disk electrode. The flow injection analysis (FIA) system consisted of a carrier reservoir, a Cole Parmer Masterflex microprocessor pump drive, a Rehodyne 7125 sample injection valve (20-μl loop), interconnecting Teflon tubing, and a BAS CC-5 type electrochemical injector.

$SiMo_{12}$ doped PPy modified films were grown on the glassy carbon electrode surface by cycling the electrode potential continuously between −0.2 and 0.65 V vs Ag/AgCl in aqueous solutions containing pyrrole, $SiMo_{12}$, and supporting electrolyte. Prior to modification, glassy carbon electrode was polished with 0.05 μm alumina on Buehler (Lake Bluff, IL, USA) felt pads and then ultrasonically cleaned for about a minute in water. Finally, the electrode was washed thoroughly with double distilled water and used. After film formation, the electrode was rinsed with distilled water and used for further characterization.

Results and discussion

Preparation of $SiMo_{12}$ doped PPy film modified electrode

Figure 1 shows typical CVs obtained by scanning electrode potential from −0.2 to 0.65 V (vs Ag/AgCl) in fresh 0.2 M H_2SO_4, solution containing pyrrole, and $SiMo_{12}$ solution. The peak currents increase with increasing cycle number, indicating that $SiMo_{12}$ is effectively doped in the matrix of
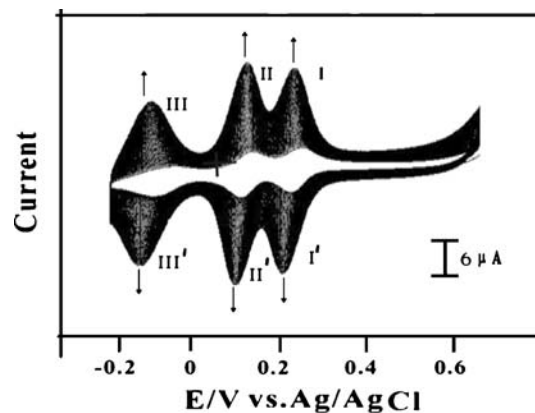

Fig. 1 CVs obtained by consecutive sweeps in 0.2 M H_2SO_4 solution containing 1×10^{-3} M $SiMo_{12}$ and 0.03 M pyrrole. Potential range −0.2 to 0.65 V. Scan rate 0.1 V/s

PPy. It can be seen clearly that, in the potential range −0.2 to +0.65 V (vs Ag/Agcl), there are three reversible redox peaks that appear, and differences of the peak potentials are all about 0.025 V, with formal potentials that are 0.22 (I), 0.10 (II), and −0.11 V (III). Redox peaks I–I′, II–II′, and III–III′ correspond to three consecutive two-electron processes for the couples of $SiMo_{12}O_{40}^{4-}$, $H_4SiMo_{12}O_{40}/H_6SiMo_{12}O_{40}$, $H_6SiMo_{12}O_{40}/H_8SiMo_{12}O_{40}$, $H_8SiMo_{12}O_{40}/H_{10}SiMo_{12}O_{40}$, which were described as follows [39, 40]:

$$H_4SiMo_{12}^{VI}O_{40} + 2H^+ + 2e^- \rightarrow H_6SiMo_{10}^{VI}Mo_2^VO_{40}$$

$$H_6SiMo_{10}^{VI}Mo_2^VO_{40} + 2H^+ + 2e^- \rightarrow H_8SiMo_8^{VI}Mo_4^VO_{40}$$

$$H_8SiMo_8^{VI}Mo_4^VO_{40} + 2H^+ + 2e^- \rightarrow H_{10}SiMo_6^{VI}Mo_6^VO_{40}$$
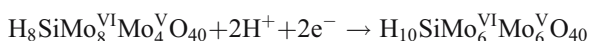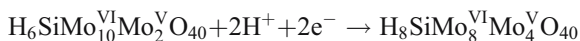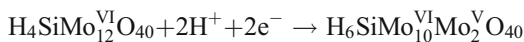
Figure 2a shows the electrochemical behavior of $SiMo_{12}$ doped PPy film compared with that in aqueous solution, and all three redox peak currents improve greatly in $SiMo_{12}$ doped PPy film modified electrode. This suggests that redox reaction of $SiMo_{12}$ anion can be mediated by the electron transfer through the PPy network, and $SiMo_{12}$ in the matrix of PPy has a faster electron transfer.
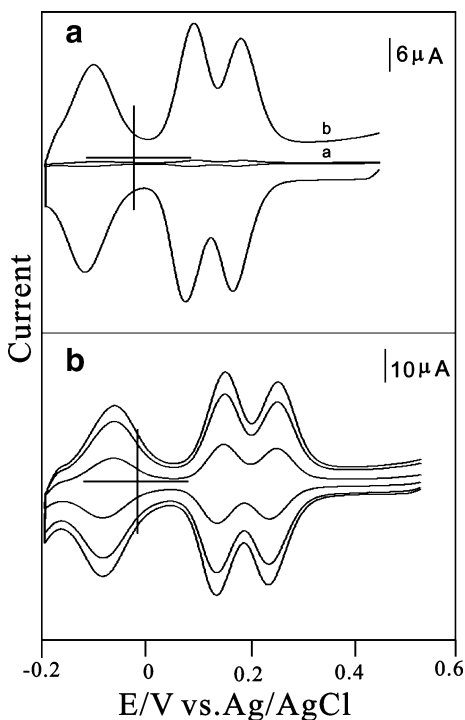
Optimal modified electrode was estimated to deliver higher catalytic current response by varying surface concentration in terms of film thickness. A coating electro-deposited from 10, 25, and 50 potential cycles is shown in Fig. 2b (from inner to outer, respectively). With 25 potential cycles, a higher current growth response is obtained than with 10 (thin) and 50 potential cycles (thick). This observation indicates that thin films probably do not offer enough catalytic site, while the thicker ones seem to suffer from a resistive barrier to the delivery of electrons.

Electrochemical characterization of $SiMo_{12}$ doped PPy film modified electrode

Figure 3a,b shows the CVs of the modified electrode at different scan rates in the potential range −0.2 to 0.65 V in 0.2 M H_2SO_4 solution. The peak currents of three redox couples are directly proportional to scan rates up to 900 mV s^{-1} (insets of Fig. 3a,b), as expected for surface-confined processes. Moreover, the ratio of oxidation-to-reduction peak currents is nearly unity, and formal potentials did not change with increasing scan rate. This result reveals that the
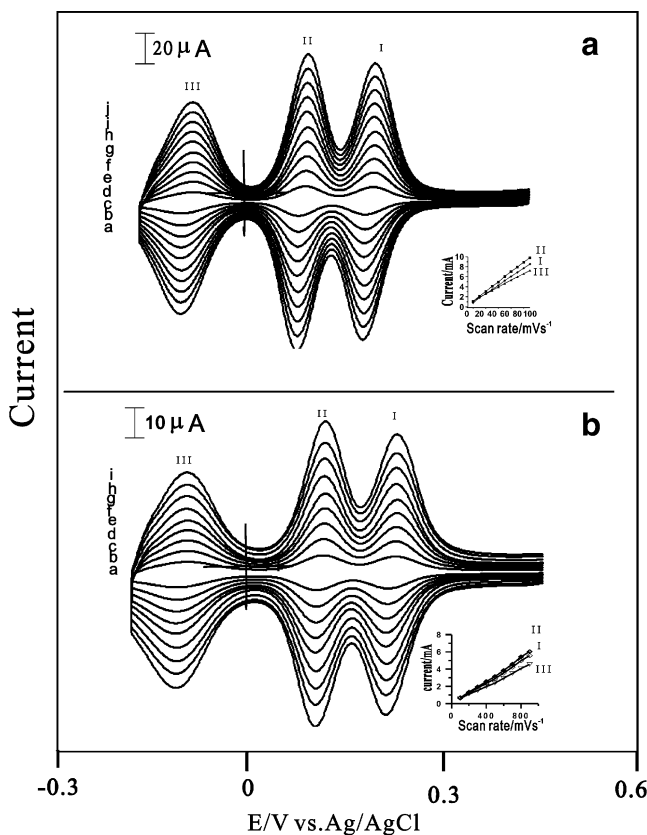

Fig. 2 a CVs of $SiMo_{12}$ doped PPy film (*a*). For comparison, the response of $SiMo_{12}$ film at bare glassy carbon electrode (*b*) is provided. Electrolyte 0.2 M H_2SO_4 solution. Scan rate 0.1 V/s. b CVs of $SiMo_{12}$ doped PPy film modified electrode in 0.2 M H_2SO_4 solution, from inner to outer, 10, 25, and 50 cycles of film thickness. Electrolyte 0.2 M H_2SO_4 solution. Scan rate 0.1 V/s

Fig. 3 a CV of $SiMo_{12}$ doped PPy film modified electrode at different scan rates; *a* 10, *b* 20, *c* 30, *d* 40, *e* 50, *f* 60, *g* 70, *h* 80, *i* 90, and *j* 100 mV/s. b *a* 100, *b* 200, *c* 300, *d* 400, *e* 500, *f* 600, *g* 700, *h* 800, and *i* 900 mV/s: *Insets*: I_{Pc} vs scan rate: electrolyte is 0.2 M H_2SO_4 solution

electron transfer kinetics is very fast in the modified electrode surface.

The charge under two reduction peaks appearing at the potentials ca. 0.22 to 0.10 V (Fig. 3a) are about 15%. The third set of seems to be already somewhat affected by the proton discharge reaction. Based on the data for second best-defined cathodic peak at 0.10 V, we have estimated, the amount of $SiMo_{12}$ doped into PPy the film (Γ_{SiMo12}) was calculated with the following equation [39]:

$$\Gamma_{SiMo\,12} = Q_t/nFA_e$$

where Q_t is the charge consumed, obtained from integrating the peak area in CVs at the scan rate of 10 mV/s, n is the number of electrons consumed ($n=2$ in the present case), and A_e is the electrode area (cm^2). In the present work, we have estimated the apparent surface coverage of $SiMo_{12}$ to be on the level of ca. 0.5×10^{-10} mol cm^{-2}.

The pH of the supporting electrolyte has a marked effect on the electrochemical behavior of the $SiMo_{12}$ doped PPy film modified electrode. Along with increasing pH, the peak potentials all gradually shift to the more negative potential direction, and the peak currents gradually decrease (Fig. 4). It can be explained by fact that the reduction of $SiMo_{12}$ doped PPy matrix was accompanied by the transfer of protons from solution to the surface of the electrode to charge neutralization (balance of charge), which, of course, is the reason for the observed current in the modified electrodes. Along with increasing pH values (replacement of H^+ by the bulky cations), slower penetration (charge propagation) of bulkier cations to the active centers should most likely be the reason for the decrease of the current. This explained the shift of more negative reduction potentials by Nernst equation [41]; when the solution was made in 0.2 M H_2SO_4 solution, the low pH voltammogram
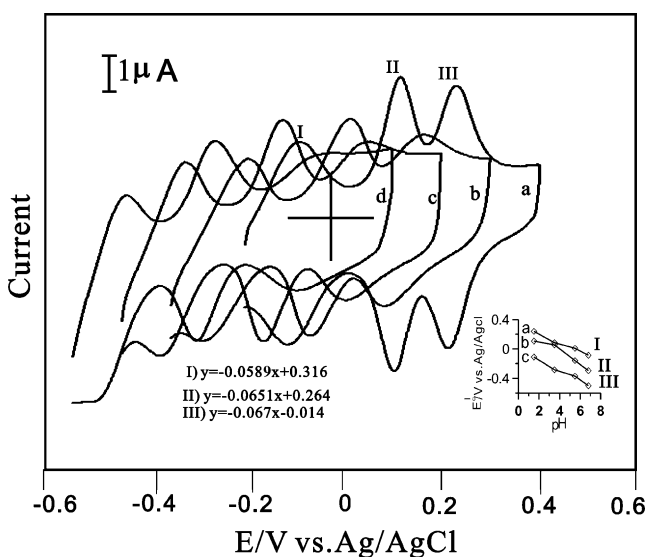
was restored. This tends to suggest that, as long as there is a high concentration of protons in the solution, charge compensation by the other cations is unnecessary, as has been observed elsewhere [25]. The formal potential-pH diagram was constructed by plotting $E^{\circ\prime}$ values as a function of pH of the solution (inset of Fig. 4). This diagram comprises a straight line with a slope of 58 (I), 65 (II), and 67 mV/pH (III). This behavior suggests that it obeyed the Nernst equation for the two electrons and two protons transfer reaction.

Electrochemical quartz crystal microbalance of study of $SiMo_{12}$ doped PPy film

Figure 5a,b shows the consecutive CVs and quartz crystal microbalance results for electropolymerziation of (0.03 M) pyrrole from the solution containing 0.2 M H_2SO_4. Figure 5a indicates an increase in the peak current of PPy film and Fig. 5b shows the change in electrochemical
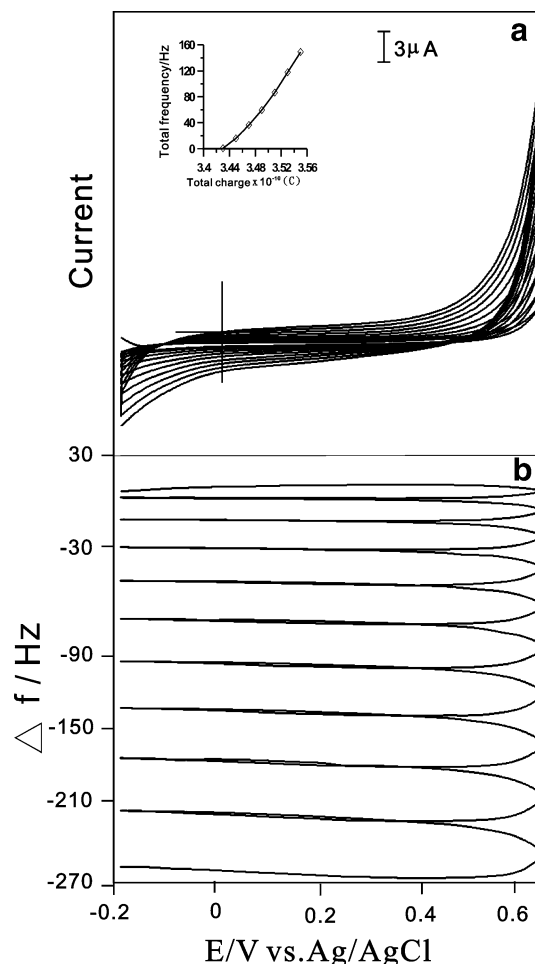
Fig. 5 a Consecutive CVs of the PPy film formation on a gold electrode surface from aqueous solution containing 0.03 M pyrrole in 0.2 M H_2SO_4 in the potential scan −0.2 to 0.65 V. b The frequency change responses recorded during the consecutive CVs between −0.2 to 0.65 V. Inset: total charge vs total frequency

Fig. 4 CVs at different pH values a 1.5, b 3.4, c 4.5, and d 5.6: Scan rate is 0.1 V/s. The inset shows $E^{\circ\prime}$ vs pH. Scan rate = 0.1 V/s

quartz crystal microbalance (EQCM) frequency during the first ten cycles of the consecutive cyclic voltammetry. These results also showed the obvious deposition potential that occurred between 0.5 and 0.65 V. The inset of Fig. 5a shows a plot of total frequency change vs total charge, and this curve was linear as expected for the Sauerbrey relation to consider rigid [42, 43].

Figure 6a,b depicts the consecutive CVs and quartz crystal microbalance results for doping of $SiMo_{12}$ ions into PPy film. During the oxidation of PPy, $SiMo_{12}$ ions were started to dope from 0.45 to 0.6 V; simultaneously, frequency decrease was detected, which implied a mass increase. However, during reduction there was no change in mass from 0.45 to −0.2 V. This indicates that, during
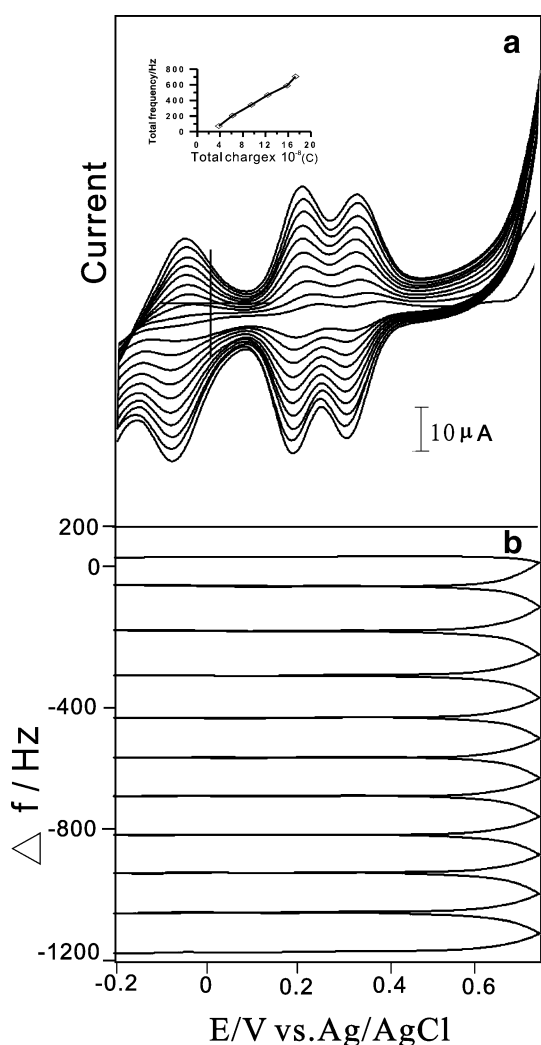

Fig. 6 a Consecutive CVs of the $SiMo_{12}$ doped PPy film formation on a gold electrode surface from aqueous solution containing 0.03 M pyrrole + 0.2 M H_2SO_4 + 1 mM $SiMo_{12}$ in the potential scan −0.2 to 0.6 V. b The frequency change responses recorded during the consecutive CVs between −0.2 and 0.6 V. Inset: total charge vs total frequency

reduction of the polymer, the charge compensation was achieved through insertion of cations from electrolyte and $SiMo_{12}$ ions were not dedoped. The inset of Fig. 6a shows a plot of total frequency change versus total charge, and this curve was linear, as expected for the Sauerbrey relation to consider rigid film [42, 43]. From the frequency change, the change in the mass during $SiMo_{12}$ ions were doped in the PPy film can be calculated by using the Sauerbrey equation.

$$Mass\ change(\Delta m) = -1/2\left(f_0^{-2}\right)(\Delta f)A(K\rho)^{1/2}$$

Here, Δf is the frequency change, A is the area of the gold disk, ρ is the density of the crystal, and f_0 is the oscillation frequency of the crystal. A 1-Hz frequency change is, however, equivalent to a 1.4-ng change in the mass. The mass change during doping of $SiMo_{12}$ ions into PPy film was found to be 1.68 $\mu g/cm^2$, and PPy film was found to be 0.378 $\mu g/cm^2$ for the first ten cycles for both experiments. From the above result, the amount of $SiMo_{12}$ anions deposited on the electrode was determined to be 1.3 $\mu g/cm^2$.

Surface morphological study of $SiMo_{12}$ doped PPy film modified electrode

Figure 7 depicts atomic force microscope (AFM) images of $SiMo_{12}$ doped PPy film on ITO surface. The film was obtained by cycling the electrode between the potential range of −0.2 to 0.65 V in an aqueous solution containing 0.2 M H_2SO_4, pyrrole, and $SiMo_{12}$. Figure 7a,b corresponds to topographic horizontal cross-section analysis and topography of $SiMo_{12}$ doped PPy film. Figure 7c corresponds to the three-dimensional version obtained for the same $SiMo_{12}$ doped PPy film. From the horizontal cross-section analysis, the maximum and minimum globule sizes were estimated to be in the range 50–200 nm. The thickness of the film was measured to be 30±10 nm. Similar types of topographic and horizontal cross-sectional analysis studies were reported to PEDOT modified electrode by Phani et al. [44].

Electrocatalytic study of $SiMo_{12}$ doped PPy film modified electrode on reduction of Cr(VI)

The determination of trace levels of Cr(VI), which are often below 1 ppb in natural waters and biological fluids in the presence of relatively high concentrations of Cr(III), is of particular importance [45]. From Fig. 8, it can be seen clearly that no obvious response was observed for Cr(VI) on the bare electrode; however, the catalytic reduction of Cr (VI) by the $SiMo_{12}$ doped PPy film modified electrode can be seen clearly: the cathodic currents increase while anodic currents decrease. The catalytic wave appears on the third
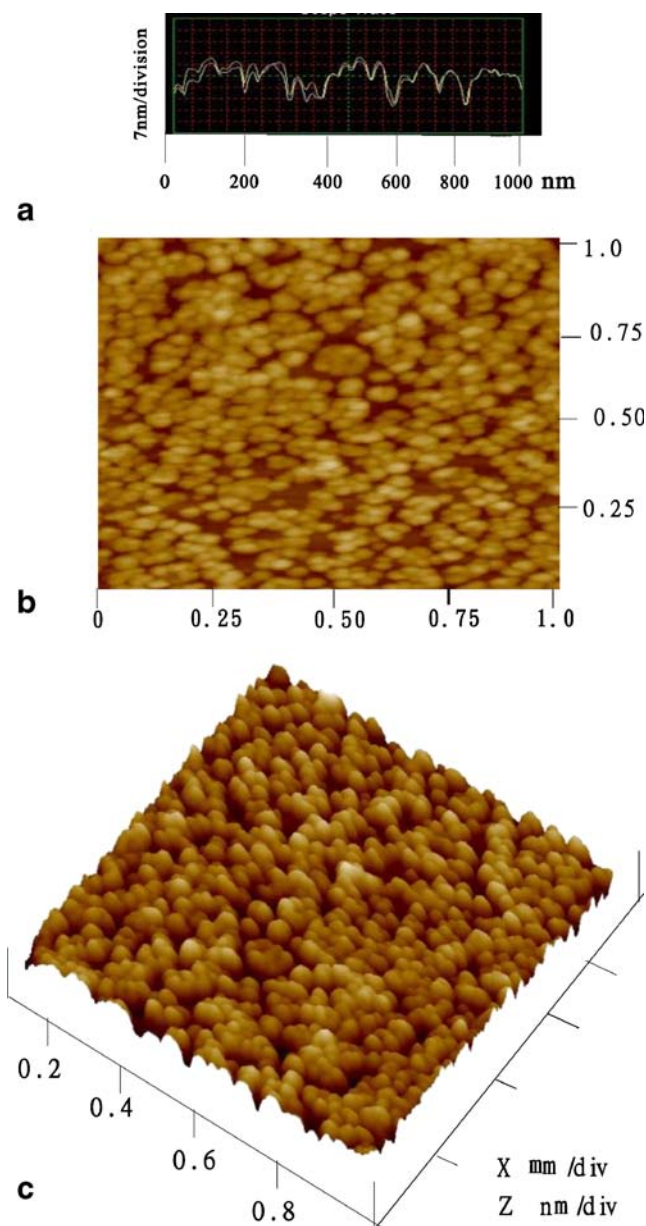
Fig. 7 The AFM image of SiMo$_{12}$ doped PPy film modified electrode. **a** Graph of horizontal cross section. **b** Horizontal cross section view of topography image. **c** Three-dimensional view of the film

reduction wave of SiMo$_{12}$, corresponding to the reduction process from two-electron-reduced species to four-electron-reduced species and from four-electron-reduced species to six-electron-reduced species, respectively. The result indicates that two- to four- and four- to six-electron-reduction product has catalytic activity toward the reduction of Cr(VI). Similar electrochemical studies were observed for removal of Cr(VI) by using Fe(II) electrode [46]. The proposed mechanism for reduction of Cr(VI) to Cr(III) by SiMo$_{12}$ doped PPy film is given by the following reactions.
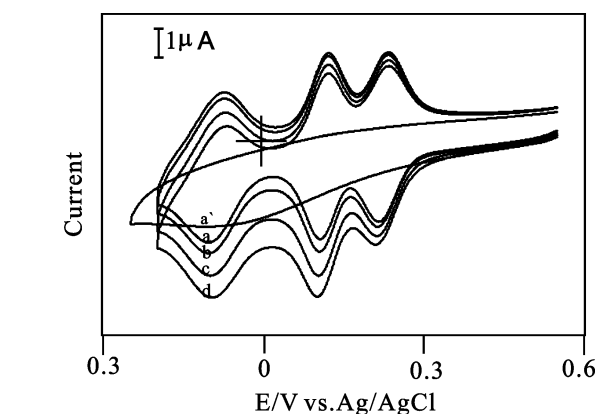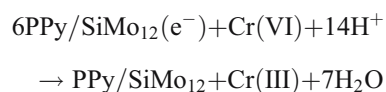

Fig. 8 CVs of Cr(VI) reduction at SiMo$_{12}$ doped PPy film modified electrode at the various concentrations a 0, b 0.1, c 0.2, and d 0.3 mM. $a^{•}$ Bare GC in the presence of 0.3 mM of Cr(VI). Solution electrolyte: 0.2 M H$_2$SO$_4$ solution. Scan rate 0.1 V/s

$$6PPy/SiMo_{12}(e^-)+Cr(VI)+14H^+$$
$$\rightarrow PPy/SiMo_{12}+Cr(III)+7H_2O$$

RDE study for SiMo$_{12}$ doped PPy film modified electrode on reduction of Cr(VI)

The electrocatalytic activity of the SiMo$_{12}$ doped PPy film modified glassy carbon electrode towards the reduction of Cr(VI) was evaluated by RDE technique also. Figure 9 presents the current–potential curves for the redox behavior of Cr(VI) at the SiMo$_{12}$ doped PPy modified glassy carbon electrode in H$_2$SO$_4$ solution at 2,500 rpm. Well defined voltammograms with a mass transport limited current were
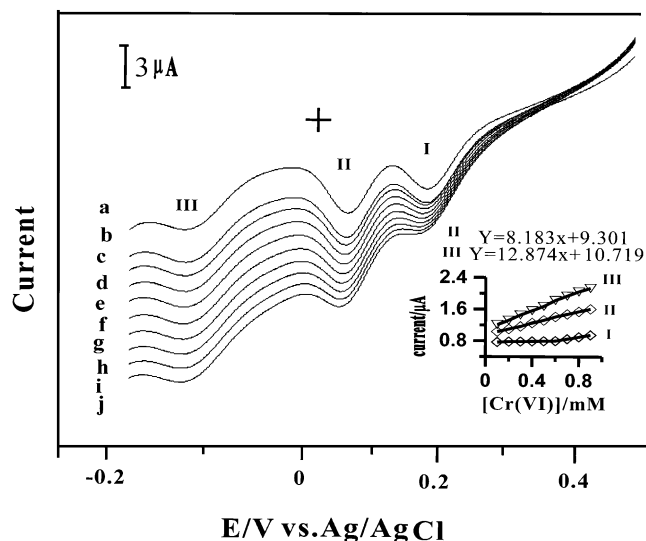

Fig. 9 RDE voltammograms of the SiMo$_{12}$ doped PPy film modified electrode in the presence of different concentrations of Cr(VI) a 0, b 0.1, c 0.2, d 0.3, e 0.4, f 0.5, g 0.6, h 0.7, i 0.8, and j 0.9 mM. *Inset* I_d vs concentrations of Cr(VI)

Table 1 Voltammetric parameters for the reduction of Cr(VI) vs surface coverage and rate constant of SiMo$_{12}$ doped PPy film modified electrode

Thickness of film (in cycles)	Peak I		Peak II		Peak II	
	$\Gamma_f \times 10^{-10}$ mol/cm^{-2}	$k_{app} \times 10^4$ M^{-1} S^{-1}	$\Gamma_f \times 10^{-10}$ mol/cm^{-2}	$k_{app} \times 10^4$ M^{-1} S^{-1}	$\Gamma_f \times 10^{-10}$ mol/cm^{-2}	$k_{app} \times 10^4$ M^{-1} S^{-1}
10	0.2	0.26	0.37	1.08	0.26	0.62
25	0.23	0.295	0.5	1.69	0.35	0.78
50	0.09	0.23	0.32	0.510	0.24	0.57

observed at each addition of Cr(VI) for peak III and II (see inset).The disc current was found increased with an increase of concentration of Cr(VI) with slope 1.3 and 0.8 μA/mM for peaks III and II, respectively.

Determination rate constant of SiMo$_{12}$ doped PPy film modified electrode by RDE

Table 1 shows the effect of the film thickness of SiMo$_{12}$ redox centers Γ and rate constant on the reduction of Cr(VI) for reduction peaks II and III. From the table, higher rate constant can be observed for 25 cycles of film thickness, and it appears to be optimal film thickness for electrocatalytic reduction of Cr(VI). Markedly, thinner (10 cycles) and thicker (50 cycles) films yield lower Cr(VI) reduction currents. The thin films probably do not offer enough catalytic sites to handle the available supply of Cr(VI), while the thicker ones seem to suffer from a resistive barrier to the delivery of electrons to the catalytic sites. A similar type of behavior is observed for electrocatalytic reduction of bromate on tungsten oxide modified electrode by Faulkner et al. [47]. Based on this trend, catalytic reaction rate constant, k, was calculated by using a Koutecky–Levich plot obtained using RDE experiment at 0.5 mM Cr(VI).

The Koutecky–Levich equation is given below:

$$I^{-1} = (nFAk_{app}\Gamma_f C)^{-1} + \left(0.620nFAD^{2/3}y^{-1/6}\omega^{1/2}C_0\right)$$

where Γ_f refers to the electrode surface coverage of SiMo$_{12}$ doped PPy calculated from the charge under the cathodic peak of SiMo$_{12}$ doped PPy reduction in cyclic voltammetric method and C is the concentration of Cr(VI); other terms have their usual meanings. From the intercept of the Koutecky–Levich plot, the catalytic reaction rate constant, k, could be found out (Table 1).

FIA Cr(VI) ions on SiMo$_{12}$ doped PPy film modified electrode

The effect of applied potential (E_{app}) was examined by fixing flow rate = 1.5 ml/min, and an optimized response was obtained upon repeated injection of Cr(VI) at $E_{app} = -0.15$ V with 0.2 M H$_2$SO$_4$ as carrier solution. The catalytic reduction current was compared between pyrrole and SiMo$_{12}$ doped

PPy film modified electrode. The result showed that SiMo$_{12}$ doped PPy film modified electrode had higher current than PPy modified electrode (Fig. 10a,b). The stability of the SiMo$_{12}$ doped PPy film modified electrode was checked by measuring peak currents obtained for 16 successive injections of a 1 μM Cr(VI) solution, the RSD being 1.6%. (Fig. 10b).
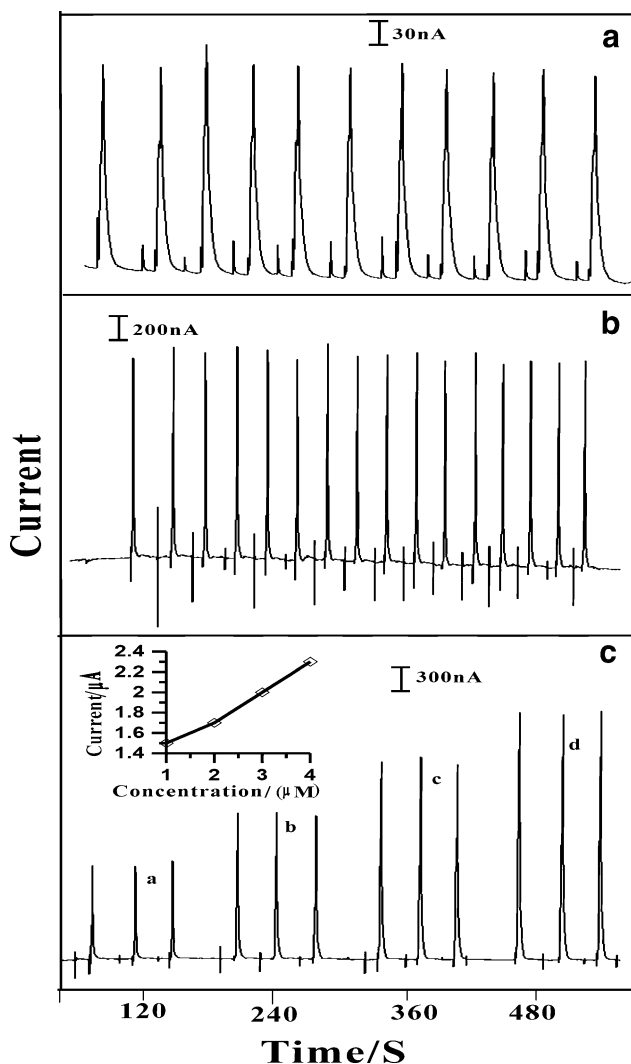

Fig. 10 **a** Current response in FIA system for PPy modified electrode for 1 μM Cr(VI) solutions. **b** Current response in FIA system for SiMo$_{12}$ doped PPy-modified electrode for 1 μM Cr(VI) solutions. **c** Current response in FIA system for SiMo$_{12}$ doped PPy-modified electrode for various concentrations of Cr(VI) *a* 1, *b* 2, *c* 3, and *d* 4 μM solutions. Carrier solution 0.2 M H$_2$SO$_4$. Flow rate 1.4 ml/min
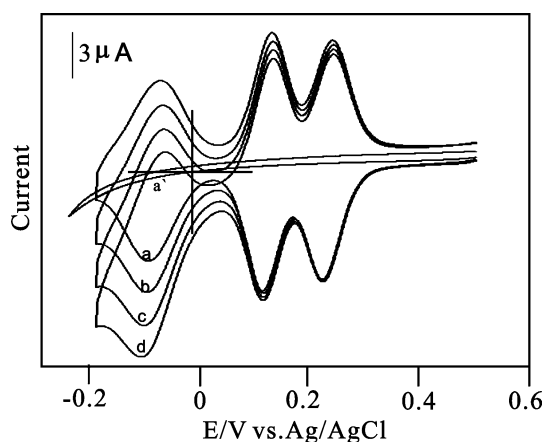
Fig. 11 **a** CVs of periodate reduction at $SiMo_{12}$ doped PPy-modified electrode at the various concentrations *a* 1, *b* 2, *c* 3, and *d* 4 mM. *a`* Bare GC in the presence of 4 mM of periodate solution. Electrolyte 0.2 M H_2SO_4 solution. Scan rate 0.1 V/s

Figure 10c showed four different micromolar concentrations of Cr(VI) to FIA response for modified electrode. The inset of Fig. 10c indicates a linear increase in the current with the slope of 0.27 µA/µM and $R^2 = 0.9918$ by addition of Cr(VI) solutions.

Electrocatalytic study of the $SiMo_{12}$ doped PPy film modified electrode on reduction of per iodate (IO_4^-)

In our experiment, we found that $SiMo_{12}$ doped PPy film modified electrode displayed electrocatalytic activity toward the reduction of periodate (Fig. 11) in 0.2 M H_2SO_4 solution in the range −0.2 to 0.5 V. It can be seen clearly that no obvious response was observed for periodate on the bare electrode; however, the catalytic reduction of periodate by the $SiMo_{12}$ doped PPy film modified electrode can be seen clearly: the cathodic currents increase while anodic currents decrease. The catalytic wave appears on the third reduction wave of $SiMo_{12}$, corresponding to the reduction process from four-electron-reduced species to six-electron-reduced species. Similar observations were made by Liu and Dong [34]. The result indicates that four- to six-electron-reduction product has catalytic activity toward the reduction of periodate.

Conclusion

The $SiMo_{12}$ doped PPy film modified electrode was prepared by electrochemical polymerization method from solution containing 0.2 M H_2SO_4, $SiMo_{12}$, and pyrrole. EQCM studies revealed that $SiMo_{12}$ doped PPy film had a rigid film. The modified electrode surface was characterized by AFM. It was found that the minimum and maximum globule sizes were estimated to be in the range

50–200 nm. The thickness of the film was measured to be 30±10 nm. The modified electrode shows good electrocatalytic activity toward reduction of Cr(VI) and periodate. Rate constants were determined by using RDE experiment to electrocatalytically reduce Cr(VI) for three different film thickness. The estimated rate constants at optimal film thickness were 0.29×10^4, 1.7×10^4, and 0.78×10^4 $M^{-1}S^{-1}$ for peaks I, II, and III, respectively.

The $SiMo_{12}$ doped PPy film electrode-based FIA system should provide an easy procedure for the analysis of the 1 µM level of Cr(VI). The modified electrode exhibited good stability during 16 successive injections of 1 µM Cr(VI) in FIA.

References

1. National Research Council (1991) Environmental epidemiology, publichealth and hazardous wastes. National Academy Press, Washington DC
2. Katz SA, Salem H (1993) J Appl Toxicol 13:217
3. Juang RS, Shiau LD (1998) Ind Eng Chem Res 37:555
4. Siddiqui BA, Sharma PP (1999) Ind J Envirom Prot 19:846
5. Hanra AM, Prabhaker S (1996) Ind J Envirom Prot 38:35
6. Gaberell M, Chin Y, Hug SJ, Sulzberger B (2003) Environ Sci Technol 37:4403
7. Griend DV, Golden JS, Arrington CA (2002) J Inorg Chem 41:7042
8. Kim C, Zhou Q, Deng B, Toronton EC, Xu H (2001) Environ Sci Technol 35:2219
9. Szulczewski MD, Helmke PA, Bleam WF (2001) Environ Sci Technol 35:1134
10. Wielinga B, Mizuba MM, Hansel CM, Fendorf S (2001) Environ Sci Technol 35:522
11. Deshpande K, Cheung S, Rao MS, Dave BC (2005) J Mater Chem 15:2997
12. Hatfield TL, Kleven TL, Pierce DT (1996) J Appl Electrochem 26:567
13. Pajeshwar K, Ibanez JG, Swain GM (1994) J Appl Electrochem 24:1077
14. Golub D, Oren Y (1989) J Appl Electrochem 19:311
15. Faldini SB, Agostinho SML, Chagas HC (1990) J Electroanal Chem 284:73
16. Wang Y, Rajeshwar K (1997) J Electroanal Chem 425:183
17. Yang YJ, Huang HJ (2001) Anal Chem 73:1377
18. Ruotolo LAM, Gubulin JC (2005) React Funct Polym 62:141
19. Ruotolo LAM, Gubulin JC (2005) Chem Eng J 110:113
20. Cox JA, Kulesza PJ (1983) Anal Chim Acta 154:71
21. Keita B, Nadjo L, Krier G, Muller JF (1987) J Electroanal Chem 223:287
22. Chang YT, Lin KC, Chen SM (2005) Electrochim Acta 51:450
23. Keita B, Nadjo L, Krier G, Muller JF (1987) J Electroanal Chem 223:287
24. Liu J, Cheng L, Liu B, Dong S (2000) Langmuir 16:7471
25. Wang P, Wang X, Zhu G (2000) Electrochim Acta 46:37
26. Bond AM, Cooper JB, Marken F, Way DM (1995) J Electroanal Chem 396:407
27. Kulesza PJ, Chojak M, Miecznikowski K, Lewera A, Malik MA, Kuhn A (2002) Electrochem Commun 4:510

28. Cheng L, Cox JA (2001) Electrochem Commun 3:281
29. Wang XL, Wang E, Lan Y, Hu CW (2002) Electroanalysis 14:1116
30. Wang XL, Kang Z, Wang E, Hu C (2002) Mater Lett 56:393
31. Liu H, He P, Li Z, Sun C, Shi L, Liu Y, Zhu G, Li J (2005) Electrochem Commun 7:1357
32. Wang P, Li Y (1996) J Electroanal Chem 408:77
33. Wang L, Xiao D, Wang E, Xu L (2005) J Colloid Interface Sci 285:435
34. Liu M, Dong S (1995) Electrochim Acta 40:197
35. Han Z, Zhao Y, Peng J, Liu Q, Wang E (2005) Electrochim Acta 51:218
36. Barth M, Lapkowski M, Lefrant S (1999) Electrochim Acta 44:217
37. Guo MD, Guo HX (2005) J Electroanal Chem 585:28
38. Chang YT, Lin KC, Chen SM (2005) Electrochim Acta 51:450
39. Bard AJ, Faulkner LR (1980) Electrochemical method fundamentals and applications. Wiley, New York
40. Brown AP, Anson FC (1977) Anal Chem 49:1589
41. Wang J (1994) Analytical electrochemistry. VCH, New York
42. Orata D, Buttry DA (1987) J Am Chem Soc 109:3574
43. Servagent S, Vieil E (1990) J Electroanal Chem 280:227
44. Senthil Kumar S, Mathiyarasu J, Phani KLN, Yegnaraman V (2006) J Solid State Electrochem 10:905
45. Rao VM, Sastri MN (1982) J Sci Ind Res 41:607
46. Mukhopadhyay B, Sundquist J, Schmitz RJ (2007) J Environ Manag 82:66
47. Kulesza PJ, Faulkner LR (1998) J Am Chem Soc 110:4905